DOI: 10.1002/ejic.200900444

Ferrocene Conjugates Containing Diarginine and Aspartic Acid: Salt Bridge Interactions in Water

Anas Lataifeh,[a] Chantelle R. Bondy,[a] and Heinz-Bernhard Kraatz*[a]

Keywords: Molecular recognition / Peptide conjugates / Amino acids / Bioorganic chemistry / Metallocenes / Electrochemistry

The ferrocene peptide conjugates of diarginine (MeO-Fc-Arg-Arg-NH_2) (**1**) and aspartic acid [Boc-Fca-Asp(OH)-OH] (**2**) were found to form a stable 1:1 associate in aqueous solution. The molecular recognition was achieved through a combination of multipoint hydrogen bonding (H-bonding) sites and a guanidinium-carboxylate ion pair. The associate stoichiometry was confirmed by using ESI-MS and NMR experiments; the NMR titration curve shows multiple equilibria with stepwise interconversion from 1:2→1:1 binding ratios, and the electrochemical behaviour of the ferrocenyl groups (Fc, Fca) confirm the formation of an ion pair. The CD spectra in the peptide region exhibit a characteristic absorption of a more ordered structure, while the ferrocene helical chirality remains intact. The solid-state IR measurements exclude the involvement of the amide backbone in the interaction.

Introduction

A wide variety of biological phenomena occur through molecular recognition in aqueous media.[1] Recognition events such as electrostatic interactions, H-bonding and hydrophobic forces all contribute to the stability of systems like (i) the secondary structure of proteins,[2] (ii) protein–substrate binding,[3] and (iii) protein–protein association for the formation of large aggregates.[4] These natural systems provide the inspiration for rational design of synthetic receptors by providing insight into the binding forces and conformational features that contribute to the formation of these associates. Salt bridges are commonly seen in Nature, where an arginine (Arg)-glutamate (Glu) pair or arginine (Arg)-aspartate (Asp) pair interacts through their guanidinium and carboxylate groups. For example, the binding site of one epitope of lysozyme reveals a formation of a salt bridge between the guanidinium of Arg68 with at least one carboxylate of Glu50 in HyHEL-5.[5] Salt bridges are also important in the activity of dihydrofolate reductase, RNA stem loops and zinc finger/DNA complexes.[6] Synthetic receptors containing a guanidinium-carboxylate H-bonding motif (see Figure 1) have been studied to provide some insight into the structure and function of such systems.[7]

Our interest in salt bridges stems from our desire to create simple biomimics of protein binding domains that guide the assembly of small peptide conjugates into well defined aggregates.[8] In this paper, we study the recognition between diarginine and aspartic acid ligands which is mediated by salt bridge formation between the guanidinyl Arg ligand and carboxylates of Asp ligand, both peptides were built on ferrocenoyl scaffolds, as shown in Figure 1. The complementarity of **1** and **2** allows for the possibility of different binding ratios such as 1:1, 1:2 and 1:3. Disubstituted ferrocene was chosen as the scaffold to enhance the rigidity of the interface by intramolecular H-bonding between the podent substituents on the cyclopentadienyl (Cp) rings (Figure 1).[9] Moreover, the difference in the electrical potential between the two ferrocenoyl units provides electrical properties that could be exploited in biologcal electron transfer (ET) chain reactions and biologcal wires.[10] Unlike

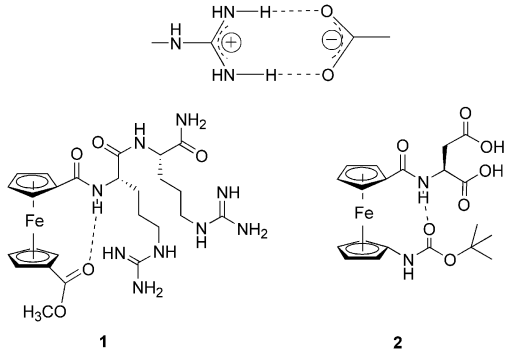

Figure 1. Schematic representation of a salt bridge formation between the guanidinium and carboxylate recognition elements of our molecules, the structure of the diarginine conjugate **1** based on ferrocene-1,1′-dicarboxylic acid (Fc), and aspartic acid conjugate **2** based on 1-aminoferrocene-1′-carboxylic acid (Fca), the intramolecular H-bond is shown as broken line.

[a] Department of Chemistry, University of Western Ontario, 1151 Richmond Street, London, Ontario, N6A 5B7, Canada
E-mail: hkraatz@uwo.ca

Supporting information for this article is available on the WWW under http://dx.doi.org/10.1002/ejic.200900444.

previous reports on molecular recognition by guanidinium-carboxylate salts bridges,[7,11] the work documented here is entirely based on biologically occurring ligands.

We designed a receptor and guest that would interact in a competitive solvent such as water. The choice of an Arg containing host arises from its ability to minimize desolvation penalties upon formation of a salt bridge,[12] this is due to the charge being dispersed over the entire guanidinium group when compared to the ammonium group found in the amino acid lysine. The more rigid Asp was chosen over the flexible Glu to reduce the possibility of supramolecular formation of ill-defined H-bonded bioorganometallic aggregates.

Results and Discussion

The ferrocene conjugates, **1** and **2** were prepared according to Scheme 1. The Fc-conjugate **1** was prepared by solid-phase peptide synthesis (SPPS) using Fmoc-Arg(Pfb)-OH, Fmoc = 9-fluorenylmethyloxycarbonyl, Pfb = 2,2,4,6,7-pentamethyldihydrobenzofuran-5-sulfonyl. The consecutive coupling of the two Arg residues and the *N*-terminal amino group of the diarginine to 1′-methoxycarbonylferrocene-1-carboxylic acid (1,*n*′-MeO-Fc-OH) was carried out using HBTU (*O*-benzotriazol-1-yl-*N*,*N*,*N*′,*N*′-tetramethyluronium hexafluorophosphate). Cleavage from the resin was accomplished using concentrated trifluoroacetic acid (TFA) with concurrent removal of Arg side-chain protecting groups. Instead of isolating the free carboxylate peptide, the *C*-terminal was amidated (Pal resin) as this prevents self-association and increases the overall aqueous solubility. The final step involved neutralizing the solution and precipitating compound **1** as an orange powder in an overall yield of 23%. The synthesis of **2** involved the coupling of 1′-(*tert*-butoxycarbonylamino)ferrocene-1-carboxylic acid (1,*n*′-Boc-Fca-OH) with H-Asp(OMe)-OMe using HBTU employing a solution-phase method. The basic ester hydrolysis of the two methyl ester groups affords the free acid **2** as an orange powder in 58% yield.

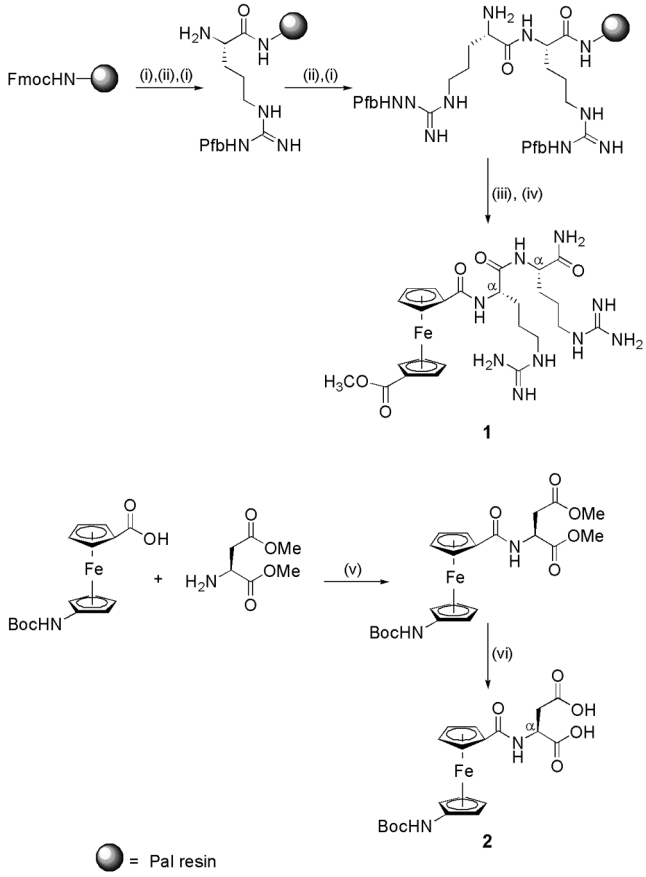

Scheme 1. Synthesis of the self-recognizing compounds **1** and **2**: (i) 20% piperidine in DMF, (ii) Fmoc-Arg(Pfb)-OH, HBTU, DMF, (iii) MeO-Fc-OH, HBTU, DMF, (iv) cleavage from resin 95:2.5:1.5:1(v/v) TFA/TIS/phenol/H_2O, (v) HBTU, CH_2Cl_2 (vi) NaOH, MeOH.

An equimolar mixture of the conjugates **1** and **2** were dissolved in a 1:1 (v/v) methanol/water solution, the resulting solution was dried to give **1·2** in quantitative yield. The original orange colour of **1** and **2** was maintained in the **1·2** associate, which is attributed to a d–d transition in the ferrocene with a λ_{max} = 444 nm (see Figure S7b in the Supporting Information). The ferrocene conjugates **1** and **2** are water-soluble while in contrast, the associate **1·2** exhibits a limited solubility in water. The structures of **1**, **2** and **1·2** were confirmed by ^{1}H NMR, ^{13}C NMR, 2D NMR, FT-IR, ESI-MS and UV(CD) spectroscopic methods. The ^{1}H NMR assignments of **1** and **2** were made on the basis of chemical shift and comparison with similar compounds (Figure S1, S2 Supporting Information). The ^{1}H and ^{13}C NMR signals produced by the cyclopentadienyl (Cp) protons of Fc and Fca moieties follow the typical signal pattern of an asymmetrical-disubstituted ferrocene (intensity ratio 2:2:2:2), where the set of *ortho* proton signals are further downfield compared to the *meta* proton signals (see Exp. Section). The ^{1}H NMR spectrum of **1·2** in [D_6]DMSO is shown in Figure S3 (Supporting Information). The Cp protons of the two components (Fc and Fca) overlap with the αCH protons of the peptide conjugates, 3.9–5.0 ppm. The NH protons of the amides and those of the Arg side chains span the region of 6.0–9.5 ppm. The 2D NMR experiments have shown weak correlations between the protons (COSY) as well as protons with carbon atoms (HSQC and HMBC) for the NH protons in **1** and **2** conjugates, surprisingly the associate **1·2** has shown a strong cross peaks in the COSY spectrum for the NH protons of the guanidinum groups at δ = 6.7 and 7.1 ppm (Figure S3 Supporting Information), this pattern of proton coupling would be expected for symmetrical end-on interaction (see Figure 1) of the carboxylate oxygen atoms with NH guanidinyl protons.[13] It was difficult to obtain reliable elemental analytical data presumably due to the associated water molecules within the solid of **1**, **2** and their associate **1·2**.

The ESI-MS spectrum of **1·2** (positive ion detection mode) was obtained from an aqueous acetone solution. The resulting spectrum, shown in Figure 2, reveals a molecular ion peak representing the [**1·2** + H]$^+$ complex at *m*/*z* = 1060.3. This is an indication of a 1:1 associate formation

in solution. High complex aggregates of **1** and **2** were not observed in the ESI-MS spectrum (Figure S4, Supporting Information). Molecular ion peaks corresponding to the monomers [**1** + H]$^+$ and [**2** + Na]$^+$ were also observed at *m*/*z* = 600.2 and 483.1, respectively.

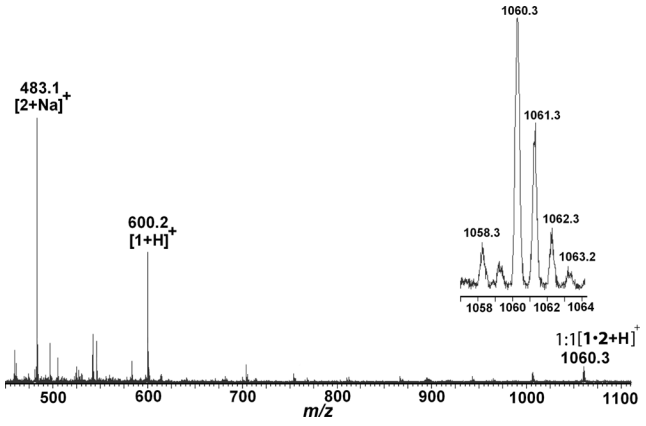

Figure 2. Typical ESI-MS spectrum of a 1:1 associate of **1**·**2** in a H_2O/acetone solution, where the peak corresponding to [**1**·**2** + H]$^+$ occurs at 1060.3 while the monomers [**2** + Na]$^+$ and [**1** + H]$^+$ produce peaks at 600.2 and 483.1, respectively.

The association properties of **1** and **2** were also studied using a ^{1}H NMR titration in a 1:4 (v/v) H_2O/[D_6]DMSO solution. Incremental addition of **2** to a solution of **1** resulted in a titration curve with a final binding ratio of 1:1. However, the data could not be fit to a simple 1:1 binding model because the titration curve "stalls" in the region of 0.5 equiv. of **2**. After this point the chemical shift continues to change until saturation is reached at approximately one equivalent of **2** added, as shown in Figure 3. This suggests the system is undergoing multiple equilibria, where an initial binding ratio of 1:2 for **1** and **2** is observed followed by a 1:1 binding stoichiometry. The binding stoichiometry was further confirmed by a Job plot obtained from the titration data (Figure S5, Supporting Information),[14d] similar findings where reported by Diederich et al. for the binding between dicarboxylates with cleft-type diamidinium receptors.[14] The presence of water has led to a significant signal broadening of the (NH) peaks in which it precluded a detailed analysis of the binding process. It was clear that distinct changes in chemical shift values were observed for a number of protons signal, in particular, those at 7.9 ppm ($\Delta\delta$ = 0.45).

The most likely binding arrangements for a 1:1 binding ratio of **1**·**2** are proposed in Figure 4. Associate **A** involves the carboxylates of Asp interacting with the side arms of the Arg residues, or to the terminal Arg residue as seen in associate **B**. The third possible mode involves binding of the Asp carboxylates to the amide backbone of **1** through H-bonds only (associate **C**). Unfortunately, no exact determination of the actual associate structure in solution was possible as no NOE (nuclear Overhauser effect) signals could be detected in the NMR spectroscopy.

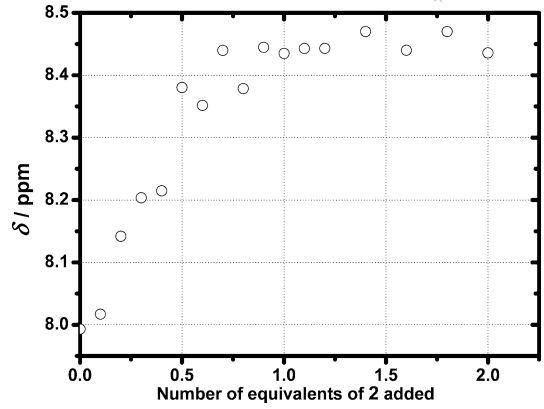

Figure 3. The change in chemical shift (δ) observed upon addition of **2** (167 mM) to a solution of **1** (34 mM) in a 1:4 (v/v) H_2O/[D_6]-DMSO solution during a ^{1}H NMR titration.

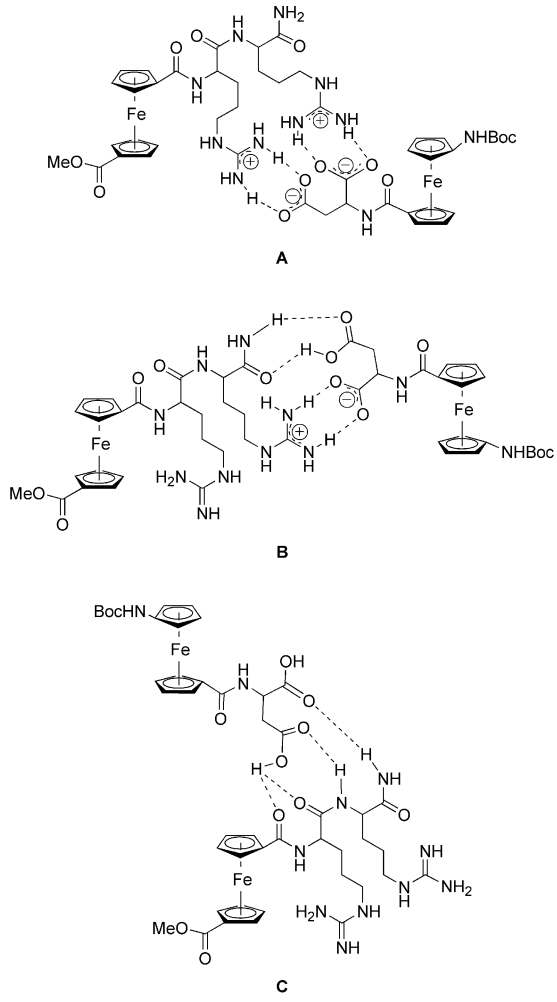

Figure 4. Proposed interactions for a 1:1 binding ratio of **1** and **2** where **A** shows a cleft binding containing two salt bridges, **B** has one salt bridge and **C** associates through multiple H-bonds to the amide backbone.

The solid-state FT-IR spectrum of **1**·**2** (Figure S6, Supporting Information) is roughly a composite absorption curve of conjugate **1** and **2** (Figure S6b) in which the ab-

sorption bands in the amide regions I and II are practically superimposable. The amide I band which arises from a $\upsilon_{C=O}$ stretching vibration with minor contribution from the C–N stretching is known to be sensitive to H-bonding. Upon interaction with H-bond donor groups, the $\upsilon_{C=O}$ stretching undergoes a shift to lower wavenumbers.[15] The spectra shown in Figure S6b demonstrate that the band due to the peptide carbonyl compounds are virtually unchanged. It is likely that the association of **1** and **2** does not involve the amide backbone (associate **C** in Figure 4).

The CD spectra of **1** and **2** in the "far-UV" region show peak minima at 217 and 214 nm, respectively. This is attributed to the absorption of the amide bond (n→π*) in L-amino acids (Figure 5).[16] A 1:1 mixture of **1** and **2** produces a new peak minimum at 221 nm showing a bathochromic shift of the amide-bond absorption. This suggests a change in the dihedral angles of the peptide backbone upon association. The CD signal of the ferrocene groups in the **1·2** associate and its monomers (**1** and **2**) does not show a change in position or helicity (λ_{max} = 560 nm, *P*-helical) see Scheme 1. However the signal intensity of **1·2** is approximately the sum of the spectra of **1** and **2** in the ferrocene region (Figure S7 in Supporting Information).

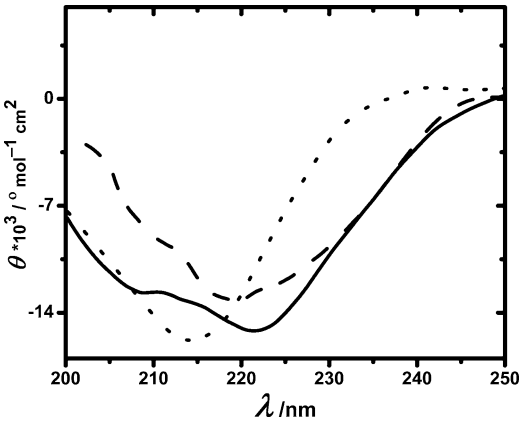

Figure 5. The CD spectra in the "far-UV" region for 1 mM of **1** (----), **2** (···) and **1·2** (—) in water, show minima at 217, 214 and 221 nm, respectively.

An explanation for our observation could be that the association does not disrupt the intramolecular interactions within the Fc-conjugates and a reorientation of the peptide backbone is required to achieve the favoured geometry of the binding interface. Hirao et al. have observed a similar effect when Pd^{II} coordinates to the pyridine nitrogen of Fc-[Ala-Pro-NHPy]$_2$, a red shift in the absorption is observed in the peptide region.[17] This was rationalized by a reorientation of the Pro amino acid allowing the formation of a compact structure, as clearly shown in the crystal structure of the Fc-[Ala-Pro-NHPyPd^{II}]$_2$ complex. Unfortunately, this result does not provide a clear picture of which associates, **A** or **B** (Figure 4), has a higher contribution to the 1:1 binding in **1·2**.

The electrochemical properties of the conjugates **1**, **2** and **1·2** were investigated using cyclic voltammetry (CV) and differential pulse voltammetry (DPV) using a glassy carbon working electrode and Pt wire as the counter electrode in an aqueous solution of 1 mM of the conjugates with $NaClO_4$ as the supporting electrolyte. A summary of the results is shown in Table 1. The Fc-conjugate **1** displays a quasi-reversible redox wave centred at $E_{1/2}$ = 437 mV (vs. Ag/AgCl), characteristic of an electrochemical step-chemical step (EC) mechanism [Figure 6, a) dashed curve]. The irreversible nature of this oxidation process presumably arises from an interaction between the lone pair on the nitrogens of the Arg ligands and the positively charged ferrocenium unit. This assumption is supported by the observation of a more reversible redox process of **1** which appears in the voltammogram of the complex **1·2**, vida supra. Similar electrochemical findings reported by Beer et al. have been observed for a ferrocene guanidinium receptors.[18] The Fca-conjugate **2** exhibits a one electron oxidation to the corresponding ferrocenium mono-cation $\mathbf{2}^+$ at $E_{1/2}$ = 175 mV [Figure 6, a) dotted curve]. The CV responses observed using scan rates ranging from 25 to 200 mV shows a quasi-reversible electrochemical process, the peak current i_{pa} increases linearly as function of $v^{-1/2}$ and the peak-to-peak separation remains constant with a current ratio close to unity (Table 1). The conjugates **1** and **2** contain two non-equivalent redox centres, this is clearly seen by the well separated redox waves. It is worth mentioning that the conjugates **1** and **2** are both shifted cathodically compared to the parent ferrocene units 1,*n*′-MeO-Fc-OH and 1,*n*′-Boc-Fca-OH, respectively due to a peptide effect (Table 1).[19]

Table 1. Electrochemical parameters for the conjugates **1**, **2** and **1·2** and the parent Fc and Fca units, detailing the shift and reversibility of the ferrocene potential as well as the change in the diffusion coefficient taken at 23 ±1 °C.

Compound	E_{pa}[a]	E_{pc}[a]	ΔE[b]	$E_{1/2}$[c]	i_{pa}/i_{pc}	D_o[d]
1	518(13)	356(12)	162	437	1.056	0.27
2	200(3)	150(4)	50	175	1.162	2.44
1·2	521(7)	488(4)	33	505	0.780	6.78
	164(8)	150(9)	14	157	0.960	2.44
MeO-Fc-OH	625(16)	513(12)	112	569	1.500	6.05
Boc-Fca-OH	319(5)	250(3)	69	285	1.600	0.65

[a] E_{pa}, E_{pc} measurements in millivolts, standard deviations are in parenthesis. [b] $\Delta E = E_{pa} - E_{pc}$. [c] $E_{1/2} = (E_{pa} + E_{pc})/2$. [d] $D_o \times 10^{-6}$ in $cm^2 s^{-1}$ determined using Randles–Sevcik equation, $i_p = 0.4463nFAC^*(nF\upsilon D_o/RT)^{1/2}$.

The complex **1·2** displays two separate redox waves [Figure 6, a) solid curve] where the more cathodic peak is ascribed to the redox process of the electron rich Fca unit of **2**. The more anodic peak is ascribed to the redox reaction of the electron deficient Fc unit of **1**. CV responses with scan rates ranging from 25 to 200 mV exhibit two quasi-reversible electrochemical processes characteristic of a bound form of **1·2**. The higher current intensity of **1** in the associated complex is due to a change in the overall reversibility of the system. An increase in the diffusion coefficient D_o of **1** was observed upon association (Table 1 and Figure S8 in Supporting Information), which is most likely due to the formation of the charged species $\mathbf{1{\cdot}2}^+$. Such a difference in the diffusion coefficient between free and associated species has been observed in ferrocyanide inclusion complexes

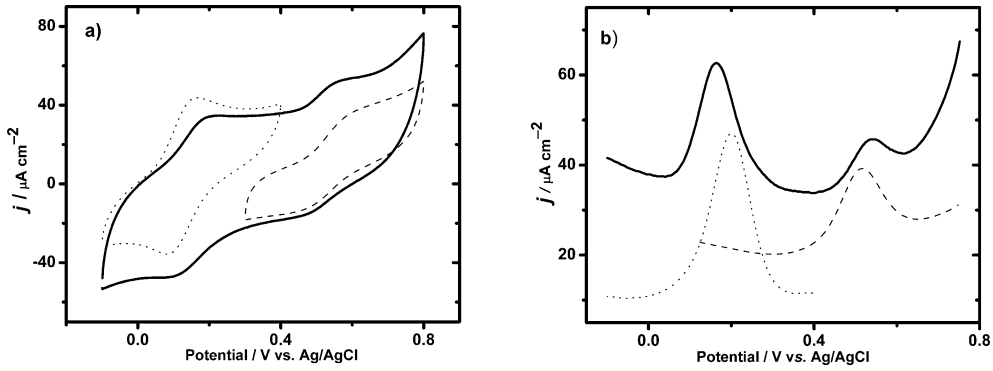

Figure 6. Typical CVs. (a) and DPVs. (b) of 1×10^{-2} mM of **1** (----), **2** (···) and **1·2** (—) in 1.0 mM aqueous solution of $NaClO_4$, glassy carbon as working electrode, Pt wire as counter electrode and Ag/AgCl as reference electrode. CVs. were recorded at 0.1 V s^{-1}, DPVs. were recorded at amplitude: 0.05 V, pulse width: 0.05 s and a pulse period: 0.2 s at 23 ± 1 °C.

of cyclodextrin and polyamine macrocycles.[20] The DPV experiments of the oxidation of **1**, **2** and **1·2** [Figure 6, b)] confirm the "shifting behaviour" of the ferrocene centres in **1·2**,[21] with a modest cathodic shift of the Fca group ($\Delta E_{1/2}$ = –18 mV). This negative shift is most likely due to an effective electric field stabilization of the positively charged Fca^+ in **1·2** by the carboxylate anion residues near the salt bridge interface ($\Delta\Delta G$ = –1.27 kJ mol^{-1}).[21]

The fact that oxidation of **2** in the 1:1 adduct **1·2** becomes easier upon association is consistent with a proton-transfer reaction.[22] This is in line with results obtained by Rotello et al. on stabilization of ferrocenium state in ferrocenecarboxylic acid by salt bridge formation with benzamidine.[22a] The redox behaviour of the more positive potential Fc unit has shifted anodically upon binding ($\Delta E_{1/2}$ = 68 mV) [Figure 6, b)]. This could be rationalized by the conformational preorganization of the peptide backbone during the binding process vide infra, which transferred to the Fc-moiety and translated as an increase in the oxidation potential,[19] as well as to the formation of positive charge at the interface. The redox signatures of Fc and Fca in the **1·2** associate did not reveal a strong electronic coupling between the ferrocene centres as proved by the observation of CV waves corresponding to the redox process of the individual ferrocene centres. This is assuming hints of "communication" between non-equivalent redox centres appear as a single redox wave signalled by a larger ΔE_p value.[23]

Conclusions

The ferrocene conjugates of diarginine **1** and aspartic acid **2** form a stable 1:1 complex in aqueous solution. The ^1H NMR titration experiment and the electrochemical measurements showed that the peptide portions of conjugates **1** and **2** are associated through H-bonding and ionic interactions. This interaction involves the reorganization of the peptide backbone as seen from the CD spectrum. However, the FTIR measurements suggest that the peptide backbone is not part of the interaction; these results form the basis for more detailed study into the structures of larger bioorganometallic architectures with potential for detection of biorecognition events.

Experimental Section

General: Ferrocene derivatives (1,*n*′-MeO-Fc-OH and 1,*n*′-Boc-Fca-OH) were prepared by standard procedures.[24] H_2N-Asp(OMe)-OMe·HCl was prepared by standard procedure from H_2N-Asp(OH)-OH and thionyl chloride.[25] H_2N-Asp(OH)-OH, Fmoc-Arg(pfb)-OH, HBTU, HOBt·H_2O (1-hydroxybenzotriazole monohydrate) and PAL resin [loading: 0.5 mmol/g, cross linking: 1% divinylbenzene (DVB)] were obtained from Advanced ChemTech. TFA, sodium sulfate anhydrous (Na_2SO_4), sodium hydrogen carbonate ($NaHCO_3$), triisopropylsilane (TIS) and thionyl chloride were used as received from VWR. Sodium perchlorate anhydrous was purchased from Alfa Aesar (ACS grade). CH_2Cl_2 (BDH, ACS grade) used for synthesis was dried (CaH_2) and distilled prior to use. Methanol (CH_3OH), acetone $(CH_3)_2CO$, hexane, ethyl acetate, chloroform, piperidine, diisopropylethylamine (DIPEA) and dimethylformamide (DMF) (BDH, ACS grade) were used as received. All syntheses were carried out in air unless otherwise stated. The column chromatography used a column of width 2.7 cm (ID) and 45 cm in length and was packed with 230–400 mesh silica gel (EM, Science). The TLC was run using aluminum plates coated with silica gel 60 F254 (EM, Science). D_2O, [D_6]acetone, [D_6]-DMSO and $CDCl_3$ (Sigma–Aldrich) were stored over molecular sieves (8–12 mesh; 4 Å effective pore size; Fisher) under inert atmosphere. Mass spectroscopy was carried out on Finnigan MAT 8200 (HRESI, HREI). UV/Vis spectra were recorded with Varian UV/Vis spectrometers.

NMR spectra were recorded with a Varian INOVA 600 MHz spectrometer using a 5 mm *z*-gradient triple resonance inverse HCX probe, operating at 600.23 MHz (^1H) and 150.78 MHz (^{13}C). Peak positions (δ) in both ^1H and (^{13}C) NMR spectra are reported in ppm relative to TMS, and coupling constants (*J*) are given in Hz. The ^1H NMR spectra are recoded with a 45° pulse angle, spectral width 9590 Hz and 128 scans and referenced to the non-deuterio impurity present in $CDCl_3$ at δ = 7.26 and in [D_6]DMSO at δ = 2.48 ppm. ^{13}C NMR spectra are recorded with a 90° pulse angle and 2 s relaxation delay, a spectral width 9590 Hz and referenced to the $CDCl_3$ signal at δ = 77.23 or [D_6]DMSO signal at δ = 40.2 ppm. ^1H NMR experiment used the excitation sculpting tech-

nique for water suppression. For the titration experiments: NMR tubes were charged with (10 mg, 0.02 mmol, 1 equiv.) of **1** at a concentration of 34 mM in 0.5 mL of 20% H_2O/[D_6]DMSO, the NMR tube was capped with septum, shaken vigorously and then injected into the spectrometer. After shimming of the magnetic field, an initial spectrum was collected, then 10 μL aliquots of H_2O/[D_6]-DMSO stock solution of conjugate **2** (0.154, 3.34×10^{-4} mmol, 20 equiv.) was added via a microsyringe (10 μL, Hamilton), the solution was then mixed by vortex, and injected into the spectrometer, the sample was reshimmed and was allowed to come to equilibrium before the next spectrum was collected. Each titration experiment was repeated at least 3 times under identical conditions.

Circular dichroism (CD) spectra were carried out with a JASCO J-810 spectropolarimeter. The spectra are an average of six accumulations between 600 to 200 nm in Millipore water at 22 ± 1 °C. The spectra were further smoothed using means-movement algorithm with convolution width of 25-point supplied with JASCO software. Ellipticity was reported as the Molar ellipticity (θ, in deg $cm^2 mol^{-1}$) and calculated as $\theta = \theta_{obs}/10lc$, where θ_{obs} is the ellipticity measured in millidegrees, c is the concentration of the sample in mol/liter (1 mM of each **1**, **2** and **1·2**), l is the optical path length of the cell in centimeters. Wavelength scans were performed in a 0.1 mm CD quartz glass cuvette.

Fourier-Transform Infrared Spectroscopy (FTIR) spectra were recoded with Impact 400 FT-IR spectrophotometer (Nicolet Analytical Instrument) at 2.0 cm^{-1} resolution at ambient temperature, using a KBr disc. The KBr pellets were prepared using a peptide ferrocene conjugate to KBr weight ratio of approximately 5:100. One thousand scans were averaged for data recorded from 400–4000 cm^{-1}; a background spectrum was collected on a dry KBr disc. To eliminate spectral contributions due to atmospheric water vapour, the KBr salt was dried in oven at 110 °C, the prepared KBr pellets were dried in a vacuum dissector, and finally the spectrometer was purged with dry N_2 upon data collection.

All electrochemical experiments were carried out at room temperature (23 ± 1 °C) using a CHI 660b voltammetric analyzer. A three-electrode cell system consisting of a glassy carbon (BAS 3.0 mm diameter) working electrode, a Pt wire as the counter electrode and Ag/AgCl (3.0 M KCl) as the reference electrode was used for the CV and DPV experiments. The carbon electrode was cleaned by polishing on micro-cloth pads with Al_2O_3 slurry (0.3 μm) and then using Al_2O_3 slurry (0.05 μm). The polished electrode was sonicated and rinsed with copious amount of Millipore water followed by washing with ethanol, drying with a Kimwipe. The background solutions (1.0 mM sodium perchlorate, $NaClO_3$) were tested before use to ensure reproducibility of the working electrode.[26] 0.01 mM solutions of MeO-Fc-OH, Boc-Fca-OH, **1**, **2** and **1·2** were prepared in 1.0 mM aqueous solution of $NaClO_3$. The solutions were degassed with argon for 2 min to ensure the complete removal of oxygen. The scan rate for DPV was 25 mVs^{-1}. iR compensation was applied to all the voltammetric measurements. For the determination of the diffusion coefficients D_o, experiments were run at scan rates 25, 50, 100, 150, 200 $mV s^{-1}$. The experiments were repeated at least 10 times to get statistical values for $E_{1/2}$.

Synthesis of MeO-Fc-Arg-Arg-NH_2 (1): The ferrocene bioconjugate was synthesized using standard SPPS and Fmoc strategy at room temperature. The resin (260 mg, 1.30 mmol) was loaded in a 10 mL syringe and was left to swell in DMF for 1 h prior to use. Removal of Fmoc group was achieved using 20% piperidine in DMF over 20 min. Peptide assembly was performed with three fold excess of the Arg amino acid (2563 mg, 3.90 mmol), with 1 min preactivation with HBTU (1438 mg, 3.90 mmol), HOBt (540 mg, 3.90 mmol) and DIPEA (0.76 mL, 4.50 mmol). Coupling of the MeO-Fc-OH (410 mg, 1.40 mmol) was performed using the same coupling protocol, after each coupling step the resin was washed with DMF (3 × 5 mL) and CH_2Cl_2 (3 × 5 mL), the coupling efficiency was monitored by the ninhydrin test. Upon the successful coupling of the ferrocene group to the peptide, the resin changed colour from off white to dark red, the resin was washed and the Fc-conjugate **1** was cleaved from the resin using a mixture of TFA, TIS, phenol and H_2O (95:2.5:1.5:1) for 1 h at room temperature. After cleavage the red colour solution was filtered and the peptide was precipitated by addition of cold diethyl ether (Et_2O). The mixture was centrifuged and the precipitate was washed with cold Et_2O and dried under N_2; yield 0.18 mg, 23%. UV/Vis (H_2O): λ = 444 nm (152 $M^{-1} cm^{-1}$). ^{1}H NMR (600.23 MHz, [D_6]DMSO, 23 °C): δ = 10.91 (m, 2 H, η1N*H*-Arg), 9.23 (br. m, 4 H, η2NH_2 Arg), 8.22 (m, 1 H, εN*H* Arg), 8.14 (m, 3 H, εN*H* Arg/CONH_2) 7.86 (m, 1 H, N*H* Arg), 7.56 (m, 1 H, N*H* Arg), 4.71 (m, 1 H, αH Arg), 4.60 (s, 2 H, CH_o Cp), 4.22 (br. s, 4 H, CH_o and CH_m Cp), 4.15 (m, 1 H, αC*H* Arg), 3.85 (br. s, 2 H, CH_m Cp), 3.65 (s, 3 H, CH_3O), 3.21 (m, 2 H, δC*Hs* Arg), 3.04 (m, 2 H, δC*H*s Arg), 2.34 (m, 2 H, βC*H*s Arg), 1.97 (m, 2 H, βC*H*s Arg), 1.34 (m, 4 H, γC*H*s Arg) ppm. ^{13}C NMR (150.78 MHz, [D_6]DMSO, 23 °C): δ = 173.0, 172.6, 172.5 (*C*=O_{amide}), 171.1 (*C*=O_{ester}), 71.8, 71.7, 71.3, 71.0, 70.0 (C Cp), 53.4 (C *C*H_3O), 48.1, 42.7, 42.5 (α*C*H Arg), 34.3, 33.9, 31.1, 30.7, 28.6 28.5, 25.6, 23.1 (*C*H_2 Arg) ppm. IR (KBr): $\tilde{\nu}$ = 3167 (br., NH_{amideA}), 1744 (s, C=O_{ester}), 1699, 1684 (vs., C=$O_{carboxyl}$), 1670, 1653, 1638 (vs., C=O_{amideI}), 1624, 1618 [s, CN(H)], 1557, 1541, 1522, 1508 (s, C=$O_{amideII}$) cm^{-1}. Pos. ESI-MS (1:1 CH_3OH/H_2O): *m*/*z* = 600.234 $[M + H]^+$; $C_{25}H_{37}FeN_9O_5$ requires 599.464.

Synthesis of Boc-Fca-Asp(OMe)-OMe: A 10 mL solution of H-Asp(OMe)-OMe (160 mg, 0.79 mmol) was added to a stirred solution of Boc-Fca-OH (250 mg, 0.70 mmol) in 40 mL CH_2Cl_2, Et_3N (0.12 mL, 0.89 mmol) and HBTU (310 mg, 0.81 mmol). The mixture was stirred for 12 h at room temperature. The solution was washed with saturated $NaHCO_3$ solution (2 × 50 mL) followed by 10% citric acid solution (1 × 50 mL) and finally with distilled water (1 × 50 mL). The organic phase was dried with Na_2SO_4 and the solvent was removed in vacuo. The final product was obtained using column chromatography; yield: 250 mg, 73%. R_f (SiO_2, hexane/ethyl acetate, 3:1) = 0.31. UV/Vis (CH_3OH): λ = 442 nm (75 $M^{-1} cm^{-1}$). ^{1}H NMR (600.23 MHz, $CDCl_3$, 23 °C): δ = 6.89 (s, 1 H, N*H*-Asp), 6.49 (s, 1 H, N*H*-Boc), 5.06 (m, 1 H, α*CH* Asp), 4.73 (s, 1 H, CH_o Cp), 4.57 (s, 2 H, CH_o Cp), 4.45 (s, 1 H, CH_o Cp), 4.37 (s, 2 H, CH_m Cp), 4.00 (s, 2 H, CH_m Cp), 3.81 (s, 3 H, CH_3O), 3.78 (s, 3 H, CH_3O), 3.10 (dd, $^2J_{H,H}$ = 16.9, $^3J_{H,H}$ = 4.92 Hz, 1 H, βC*H* Asp), 2.95 (dd, $^2J_{H,H}$ = 17.3, $^3J_{H,H}$ = 4.62 Hz, 1 H, βC*H* Asp), 1.50 (s, 9 H, Boc) ppm. ^{13}C NMR (150.78 MHz, $CDCl_3$, 23 °C): δ = 172.2, 171.9 (*C*=O_{ester}), 169.8 (*C*=O_{Fc}), 153.6 (*C*=$O_{urethane}$), 97.4 (C_{ipso} Cp), 80.3 [$(CH_3)_3C$ Boc], 76.3 (C_{ipso} Cp), 71.6, 69.8, 66.0, 65.8, 62.9, 62.2 (C Cp), 53.1, 52.3 (C *C*H_3O), 48.7 (α*C*H Asp), 36.6 (β*C*H_2 Asp), 28.5 [$(CH_3)_3$C Boc] ppm. IR (KBr): $\tilde{\nu}$ = 3348, 3275 (br. s, $NH_{amide\ A}$), 1734 (s, (C=O_{ester}), 1719 (s, C=$O_{urethane}$) 1628 (s, C=$O_{amide\ I}$), 1541 (s, C=$O_{amide\ II}$) cm^{-1}. EI-MS (CH_3OH): *m*/*z* = 488.2 $[M]^+$, 388.1 $[(M – boc) + H]^+$. $C_{22}H_{28}FeN_2O_7$ requires 488.3.

Synthesis of Boc-Fca-Asp(OH)-OH (2): Boc-Fca-Asp(OMe)-OMe (630 mg, 1.30 mmol) was dissolved in 10 mL of methanol, NaOH (120 mg, 3.00 mmol) was added and the solution was kept at room temperature for 6 h. The solution then was diluted with 50 mL water, washed with CH_2Cl_2 to remove the unreacted starting material, the solution then neutralized with 1.0 M HCl to pH 3.0 and extracted with ethyl acetate (3 × 70 mL). The combined extracts were dried with Na_2SO_4 and the solvent was removed in vacuo.

The desired product was obtained using column chromatography; yield: 300 mg, 58%; R_f (SiO_2, chloroform/methanol/acetic acid, 8.5:1:0.5) = 0.30. UV/Vis (H_2O): λ = 442 nm (114 $M^{-1}cm^{-1}$). ^1H NMR (600.23 MHz, [D$_6$]DMSO, 23 °C): δ = 8.66, 8.48 (br. s, 2 H, COO*H*-Asp), 7.11 (s, 1 H, N*H* Asp), 6.53 (s, 1 H, N*H* Boc), 4.73 (br. s, 1 H, CH_o Cp), 4.53 (br. s, 2 H, CH_o Cp and αH Asp), 4.22 (br. s, 2 H, CH_o Cp), 3.92 (br. s, 2 H, CH_m Cp), 3.46 (br. s, 4 H, CH_m Cp and βH Asp), 1.43 [s, 9 H, (CH_3)$_3$C] ppm. ^{13}C NMR (150.78 MHz, [D$_6$]DMSO, 23 °C): δ = 197.3 (*C*=O$_{carboxyl}$), 171.0 (*C*=O$_{Fc}$), 153.1 (*C*=O$_{urethane}$), 97.4 (C$_{ipso}$ Cp), 80.2 [(CH$_3$)$_3$*C* Boc], 72.1, 66.3, 65.8, 62.0 (C Cp), 48.6 (α*C*H Asp), 36.6 (β*C*H$_2$ Asp), 29.0 [(*C*H$_3$)$_3$C Boc] ppm. IR (KBr): $\tilde{\nu}$ = 2400–2248 (br., OH$_{carboxyl}$), 3117–3182 (br., NH$_{amide\ A}$), 1717 (m, C=O$_{urethane}$), 1699, 1686 (s, C=O$_{carboxyl}$), 1647 (s, C=O$_{amide\ I}$), 1557 (s, C=O$_{amide\ II}$) cm^{-1}. Pos. ESI-MS (H_2O): *m*/*z* = 943.2 [2M + Na]$^+$, 483.1 [M + Na]$^+$, 383.0 [(M – boc) + Na]$^+$. $C_{20}H_{24}FeN_2O_7$ requires 460.2.

Synthesis of 1·2: A methanol/water solution (1 mL, 1:1) of **2** (2.3 mg, 5×10^{-3} mmol) was added to a methanol/water solution (1 mL, 1:1) of **1** (3.0 mg, 5×10^{-3} mmol) and stirred at room temperature for 2 h. The solvent volume was reduced to 1 mL and the remaining solution was freeze-dried overnight to yield a pale orange powder of **1·2** in quantitative yields. UV/Vis (H_2O): λ = 444 nm (128 $M^{-1}cm^{-1}$). ^1H NMR (600.23 MHz, [D$_6$]DMSO, 23 °C): δ = 9.34 (m, 1 H, N*H* Arg), 7.91 (s, 1 H, N*H*), 7.15 (m, 2 H, N*H* Asp & N*H* Arg), 6.75 (m, 3 H, N*H* Arg), 6.37 (s, 2 H, N*H* Arg), 6.18 (m, 1 H, N*H* Boc), 4.79 (m, 1 H, αC*H*), 4.74 (m, 2 H, Cp), 4.61 (m, 2 H, Cp), 4.59 (m, 1 H, αC*H*), 4.40 (m, 4 H, Cp), 4.23 (m, 4 H, Cp), 3.94 (m, 4 H, Cp), 3.73 (s, 2.58, CH_3O), 3.61 (br. s, 4 H, δC*H* Arg), 2.89 (s, 2 H, βC*H*), 2.87 (s, 2 H, βC*H*), 2.73 (s, 2 H, βC*H*), 2.67 (m, 2 H, βC*H*), 2.33 (s, 1 H, γC*H*), 2.85 (br. s, 2 H, γH), 2.00 (s, 1 H, γC*H*) 1.97 (s, 1 H, γC*H*), 1.88 (br. s, 2 H, γC*H*), 1.43 [s, 9 H, (CH_3)$_3$C Boc] ppm. ^{13}C NMR (150.78 MHz, [D$_6$]-DMSO, 23 °C): δ = 173.3, 173.2, 172.6, 172.5 (*C*=O$_{amide}$), 170.3 (*C*=O$_{ester}$), 75.1, 73.2, 73.0, 71.8, 71.7, 71.3, 71.0, 70.0 (C Cp), 53.4 (C *C*H$_3$O), 49.6, 48.1, 42.5 (α*C*H Asp and Arg), 34.3, 33.9, 31.1, 30.7, 28.6 28.5, 25.6, 23.1 (*C*H$_2$ Asp and Arg) ppm. IR (KBr): $\tilde{\nu}$ = 3350 (s, H$_{amide\ A}$), 3180 (br. s, NH), 1734 (m, C=O$_{ester}$), 1717 (m, C=O$_{urethane}$), 1699, 1684 (vs., C=O$_{carboxyl}$), 1674, 1655, 1636 (vs, C=O$_{amide\ I}$), 1624, 1618 [s, CN(H)], 1557, 1541, 1522, 1508 (vs) (C=O$_{amide\ II}$) cm^{-1}. Pos. ESI-MS (1:1 acetone/H_2O): *m*/*z* (%) = 1060.30 [M + H]$^+$. $C_{45}H_{61}Fe_2N_{11}O_{12}$ requires 1059.72.

Supporting Information (see also the footnote on the first page of this article): NMR spectrum of **1·2** and partial 2D COSY of **1·2** in the amide region, the extended MS spectrum of **1·2** in the NH region. IR spectra of **1**, **2** and **1·2**.

Acknowledgments

This work was funded by Natural Sciences and Engineering Research Council of Canada (NSERC). We also appreciate the financial support from the University of Western Ontario (UWO). We are grateful to Lee-Ann Briere for the help with the CD measurements and to Keith Brown for the help in performing the water suppression experiments.

[1] a) G. V. Oshovsky, D. N. Reinhoudt, W. Verboom, *Angew. Chem. Int. Ed.* **2007**, *46*, 2366–2393; b) F. Hof, S. L. Craig, C. Nuckolls, J. Rebek, *Angew. Chem. Int. Ed.* **2002**, *41*, 1488–1508.

[2] a) S. Kawamura, I. Tanaka, N. Yamasaki, M. Kimura, *J. Biochem.* **1997**, *121*, 448–455; b) B. M. P. Huyghues-Despointes, R. L. Baldwin, *Biochemistry* **1997**, *36*, 1965–1970.

[3] a) Y. Jiang, V. Ruta, J. Chen, A. Lee, R. Mackinnon, *Nature* **2003**, *423*, 42–48; b) B. S. Zhorov, V. S. Ananthanarayanan, *Arch. Biochem. Biophys.* **2000**, *375*, 31–49; c) J. E. Porter, D. M. Perez, *J. Pharmacol. Exp. Ther.* **2000**, *292*, 440–448; d) O. Shoji, T. Fujishiro, H. Nakajma, M. Kim, S. Nagano, Y. Shiro, Y. Watanbe, *Angew. Chem. Int. Ed.* **2007**, *46*, 3656–3659.

[4] W. E. Stites, *Chem. Rev.* **1997**, *97*, 1233–1250.

[5] a) W. Somers, M. Ultsch, A. M. de Vos, A. A. Kossiakoff, *Nature* **1994**, *372*, 478–481.

[6] a) J. D. Puglisi, L. Chen, A. D. Frankel, J. R. Williamson, *Proc. Natl. Acad. Sci. USA* **1993**, *90*, 3680–3685; b) N. P. Pavletich, C. O. Pabo, *Science* **1991**, *252*, 809–812.

[7] a) C. Schmuck, V. Bickert, *Org. Lett.* **2003**, *5*, 4579–4581; b) C. Schmuck, M. Heil, *ChemBioChem* **2003**, *4*, 1232–1238; c) E. Fan, S. A. Van Arman, S. Kincaid, A. Hamilton, *J. Am. Chem. Soc.* **1993**, *115*, 369–370; d) K. A. Schug, W. Linder, *Chem. Rev.* **2005**, *105*, 67–114; e) F. P. Schmidtchen, M. Berger, *Chem. Rev.* **1997**, *97*, 1609–1646; f) S. Kubik, *Chem. Soc. Rev.* **2009**, *38*, 585–605.

[8] a) D. K. Smith, A. R. Hirst, C. S. Love, J. G. Hardy, S. V. Brignell, B. Huang, *Prog. Polym. Sci.* **2005**, *30*, 220–293; b) U. Boas, S. H. M. Söntjens, K. J. Jensen, J. B. Christensen, E. W. Meijer, *ChemBioChem* **2002**, *3*, 433–439; c) E. R. Gillies, J. M. J. Fréchet, *J. Org. Chem.* **2004**, *69*, 46–53.

[9] a) S. Djakovič, D. Siebler, M. Ć. Semenčić, K. Heinze, V. Rapič, *Organometallics* **2008**, *27*, 1447–1453; b) J. Lopić, D. Siebler, K. Heinze, V. Rapič, *Eur. J. Inorg. Chem.* **2007**, 2014–2024; c) D. R. Van Staveren, N. Metzler-Nolte, *Chem. Rev.* **2004**, *104*, 5931–5985; d) H.-B. Kraatz, *J. Inorg. Organomet. Polym. Mater.* **2005**, *15*, 83–106.

[10] a) H. Sun, J. Steeb, A. E. Kaifer, *J. Am. Chem. Soc.* **2006**, *128*, 2820–2821; b) R. I. Cukier, *J. Phys. Chem.* **1995**, *99*, 16101–16115.

[11] a) F. Otón, A. Espinosa, A. Tárraga, C. R. De Arellano, P. Molina, *Chem. Eur. J.* **2007**, *13*, 5742–5752; b) C. Schmuck, L. Geiger, *J. Am. Chem. Soc.* **2004**, *126*, 8898–8899; c) S. Rensing, T. Schrader, *Org. Lett.* **2002**, *4*, 2161–2164; d) M. Rekharsky, Y. Inoue, S. Tobey, A. Metzger, E. Anslyn, *J. Am. Chem. Soc.* **2002**, *124*, 14959–14967; e) J. Raker, T. E. Glass, *J. Org. Chem.* **2002**, *67*, 6113–6116.

[12] E. S. Thompson, D. B. Smithrud, *J. Am. Chem. Soc.* **2002**, *124*, 442–449.

[13] W. D. Morgan, B. Birdsall, P. M. Nieto, A. R. Gargaro, J. Feeney, *Biochemistry* **1999**, *38*, 2127–2134.

[14] a) L. Sebo, F. Diederich, *Helv. Chim. Acta* **2000**, *83*, 93–113; b) L. Sebo, B. Schweizer, F. Diederich, *Helv. Chim. Acta* **2000**, *83*, 80–92; c) S. Camiolo, P. A. Gale, M. I. Ogden, B. W. Skelton, A. H. White, *J. Chem. Soc. Perkin Trans. 2* **2001**, 1294–1298; d) K. A. Connors in *Binding Constants. The Measurement of Molecular Complex Stability*, Wiley-VCH, New York, **1987**, pp. 21–101.

[15] a) P. Saweczko, G. D. Enright, H.-B. Kraatz, *Inorg. Chem.* **2006**, *45*, 4409–4419; b) M. Iwaki, N. P. J. Cotton, P. G. Quirk, P. R. Rich, J. B. Jackson, *J. Am. Chem. Soc.* **2006**, *128*, 2621–2629; c) A. Polyanichko, H. Wieser, *Biopolymers* **2005**, *78*, 329–339.

[16] a) J. E. Forman, R. E. Barrans, D. A. Dougherty, *J. Am. Chem. Soc.* **1995**, *117*, 9213–9228; b) G. Gottarelli, S. Lena, S. Masiero, S. Pieraccini, G. Spada, *Chirality* **2008**, *20*, 471–485.

[17] T. Moriuchi, K. Yoshida, T. Hirao, *Organometallics* **2001**, *20*, 3101–3105.

[18] P. D. Beer, M. G. B. Drew, D. K. Smith, *J. Organomet. Chem.* **1997**, *543*, 259–261.

[19] H.-B. Kraatz, D. M. Leek, A. Houmam, G. D. Enright, J. Lusatyk, D. D. M. Wayner, *J. Organomet. Chem.* **1999**, *589*, 38–49.

[20] L. A. Godínez, J. Lin, M. Muñoz, A. W. Coleman, A. E. Kaifer, *J. Chem. Soc. Faraday Trans.* **1996**, *92*, 645–650.

[21] DPV removes the effect of electrode capacitive charging, resulting in measurements of only the Faradic process and hence in much higher signals than conventional voltammetries. Cal-

culated using: $\Delta\Delta G = -nF\Delta E_{1/2}$, where n is the number of electrons, involved in the process, F is the faraday constant and $\Delta E_{1/2}$ is the change in the half-wave potential following association: A. J. Bard, L. R. Faulkner, in: *Electrochemical Methods Fundamentals and Applications*, Wiley, New York, **2001**, 2nd ed, pp. 293–301.

[22] a) G. Cooke, F. M. A. Duclairoir, A. Kraft, G. Rosair, V. M. Rotello, *Tetrahedron Lett.* **2004**, *45*, 557–560; b) H. Miyaji, G. Gasser, S. J. Green, Y. Molard, S. M. Strawbridge, J. H. Tucker, *Chem. Commun.* **2005**, 5355–5375; c) C. Bourgel, A. S. F. Boyel, G. Cooke, H. A. De Cremisers, F. M. A. Duclairoir, V. M. Rotello, *Chem. Commun.* **2001**, 1954–1955.

[23] a) F. Otón, A. Tárraga, P. Molina, *Org. Lett.* **2006**, *8*, 2107–2110; b) J. Alvarez, T. Ren, A. E. Kaifer, *Organometallics* **2001**, *20*, 3543–3549.

[24] L. Barišić, V. Rapić, V. Kovač, *Croat. Chim. Acta* **2002**, *75*, 199–210.

[25] M. Brenner, W. Huber, *Helv. Chim. Acta* **1953**, *36*, 1109–1114.

[26] S. Ranganathan, T.-C. Kuo, R. L. McCeery, *Anal. Chem.* **1999**, *71*, 3574–3580.

Received: May 16, 2009
Published Online: September 2, 2009

